Microtubule inhibitors identified through non-biased screening enhance DNA transfection efficiency by delaying p62-dependent ubiquitin recruitment

Megumi Tsuchiya[1#], Hidesato Ogawa[1#]*, Kento Watanabe[1], Takako Koujin[2], Chie Mori[2], Kazuto Nunomura[3], Bangzhong Lin[3], Akiyoshi Tani[3], Yasushi Hiraoka[1,2], and Tokuko Haraguchi[1,2]*

[1]Graduate School of Frontier Biosciences, Osaka University, 1-3 Yamadaoka, Suita 565-0871, Japan

[2]Advanced ICT Research Institute Kobe, National Institute of Information and Communications Technology, 588-2 Iwaoka, Iwaoka-cho, Nishi-ku, Kobe 651-2492, Japan

[3]Graduate School of Pharmaceutical Science, Osaka University, 1-6 Yamadaoka, Suita 565-0871, Japan

# These authors contributed equally to this manuscript.

*Correspondence should be addressed to:

Hidesato Ogawa, Tel: +81 668794621; Fax: +81 668794622

E-mail address: hidesato@fbs.osaka-u.ac.jp

Tokuko Haraguchi, Tel: +81 668794621; Fax: +81 668794622

E-mail address: haraguchi@fbs.osaka-u.ac.jp

Short title: MT drugs enhance transfection efficiency

Abstract

Ectopic gene expression is an indispensable tool in biology and medicine, but is often limited by the low efficiency of DNA transfection. We previously reported that depletion of the autophagy receptor p62/SQSTM1 enhances DNA transfection efficiency by preventing the degradation of transfected DNA. Therefore, p62 is a potential target for drugs to increase transfection efficiency. To identify such drugs, a non-biased high-throughput screening was applied to over 4,000 compounds from the Osaka University compound library, and their p62-dependency was evaluated. The top-scoring drugs were mostly microtubule inhibitors, such as colchicine and vinblastine, and all of them showed positive effects only in the presence of p62. To understand the p62-dependent mechanisms, the time required for p62-dependent ubiquitination, which is required for autophagosome formation, was examined using polystyrene beads that were introduced into cells as materials that mimicked transfected DNA. Microtubule inhibitors caused a delay in ubiquitination. Furthermore, the level of phosphorylated p62 at S405 was markedly decreased in the drug-treated cells. These results suggest that microtubule inhibitors inhibit p62-dependent autophagosome formation. Our findings demonstrate for the first time that microtubule inhibitors suppress p62 activation as a mechanism for increasing DNA transfection efficiency and provide solutions to increase efficiency.

Keywords: high-throughput screening; transfection efficiency; autophagy; p62; phosphorylation; ubiquitination; gene delivery

47 **Introduction**

48 Gene delivery is one of the most important steps in gene therapy and genetic
49 modification in basic science. Gene therapy has great potential in clinical medicine, and
50 this concept has become well established in therapeutic approaches. In basic science,
51 DNA transfection is a powerful tool that enables the study of gene functions and their
52 products in cells.

53 Endocytosis is a crucial pathway for the regulation of cellular uptake of
54 plasmid DNA (Rejman *et al.* 2005; Khalil *et al.* 2006; Midoux *et al.* 2008). Importantly,
55 endocytosis can promote the induction of selective autophagy, also called xenophagy
56 (Chen *et al.* 2014). Generally, autophagy is a cytosolic bulk degradation pathway for the
57 recycling of biomolecules through nonspecific degradation of proteins and organelles
58 under nutrient starvation conditions. In contrast, selective autophagy plays an important
59 defensive role against cellular infection by pathogens, as part of a starvation-
60 independent autophagic defense system (Nakatogawa *et al.* 2009; Mizushima *et al.*
61 2011; Galluzzi *et al.* 2017). The conjugation of ubiquitin (Ub) to target pathogens is an
62 important initial process in selective autophagy. Ubiquitination assists in the recruitment
63 of autophagy receptor proteins, including p62/sequestosome-1 (p62/SQSTM1), against
64 pathogens or transfected DNA (Dupont *et al.* 2010; Roberts *et al.* 2013; Chen *et al.*
65 2014; Alomairi *et al.* 2015; Tsuchiya *et al.* 2016). Therefore, suppression of the
66 autophagy pathway can be a target for drugs to increase transfection efficiency.

67 We have previously reported that the depletion of the p62/SQSTM1 protein
68 (hereafter designated p62) greatly increases the efficiency of DNA transfection in
69 cultured cells (Tsuchiya *et al.* 2016). To monitor the behavior of the transfected DNA,
70 we developed an experimental system using DNA-conjugated beads that mimic the

71 transfected DNA. In this system, DNA-conjugated beads together with pHrodo, a
72 fluorescent marker for endosome rupture, were incorporated into cells, and their
73 intracellular dynamics were analyzed in a live cell (Tsuchiya *et al.* 2016). Using this
74 system, we demonstrated that the transfected DNA was incorporated into cells through
75 endocytosis, released from the endosomes into the cytosol, and entrapped via autophagy
76 in a p62-dependent manner. Furthermore, we demonstrated that the recruitment of Ub
77 around the transfected material was significantly delayed in p62 gene-knockout murine
78 embryonic fibroblast (p62KO-MEF) cells compared with that in normal MEF cells
79 (Tsuchiya *et al.* 2018). Additionally, p62 phosphorylation at S405 (equivalent to human
80 S403) is a crucial step for the recruitment of Ub to the target site of transfected materials
81 that mimic ectopic DNA (Tsuchiya *et al.* 2016). Hence, p62 phosphorylation at S405 is
82 an essential step for transfection-induced selective autophagy (Tsuchiya *et al.* 2018). As
83 p62 plays an important role in gene delivery through initial ubiquitination of the
84 transfected DNA, inhibition of p62 may increase transfection efficiency. The aim of this
85 study was to identify a small chemical compound that blocks the initial step of p62-
86 dependent selective autophagy to enhance DNA transfection efficiency in mammalian
87 cells.
88
89 **Results**
90 **High-throughput screening for drugs enhancing transfection efficiency**
91 To identify potential compounds that can enhance transfection efficiency, high-
92 throughput screening based on a luciferase assay was performed on MEF cells using an
93 automated workstation (Fig. 1A). The MEF cells were seeded in 384-well plates and
94 incubated for 18 h with each compound from the Osaka University compound library

95 (4,400 compounds; Tachibana *et al.* 2018) at a final concentration of 10 μM. The
96 negative control was dimethyl sulfoxide (DMSO) at a final concentration of 1%. The
97 cells were transfected with the pCMV-Luc plasmid (encoding luciferase driven by the
98 cytomegalovirus immediate early (CMV-IE) promoter) for 28 h using Lipofectamine
99 2000. The cells were subjected to a cell viability assay, followed by a luciferase assay
100 (Fig. 1A). Luciferase activity, as expressed from the transfected plasmid, was measured,
101 and transfection efficiency was evaluated based on luciferase activity normalized to cell
102 viability. Among the 4,400 compounds tested, 160 were removed from the list for
103 selection as valid compounds because of severe defects in cell morphology. The
104 transfection efficiency of the cells treated with each of the remaining 4,240 compounds
105 is plotted in Fig. 1B. In this first screening, out of the 4,240 tested compounds, we
106 identified 87 compounds that increased luciferase activity compared with that in the
107 negative control (approximately 2.1% positive hit rate). The cutoff value used for
108 selection was the mean value of the DMSO control + 4 × standard deviation (SD) (mean
109 0.347, SD = 0.242).
110 The activities of these 87 compounds were further analyzed via a second
111 screening. To achieve this, MEF cells were cultured in 96-well plates and transfected
112 with the pCMV-Luc plasmid for 28 h using Lipofectamine 2000 in the presence of each
113 of these compounds at a concentration of 1 μM (Fig. 2A). Transfection efficiency was
114 determined by a luciferase assay, in which luciferase activity expressed from the
115 transfected plasmid was measured and normalized to cell viability, as described in
116 Experimental procedures. The transfection efficiency values for the 87 compounds are
117 listed in Table S1. Notably, the top 9 compounds with high transfection efficiencies (>
118 20-fold that of the negative control) were all microtubule inhibitors (Fig. 2B; Table S1).

119 As microtubule inhibitors were found to increase transfection efficiency, we
120 also tested nocodazole, an extensively used microtubule inhibitor, which was not
121 included in the Osaka University compound library. Transfection efficiency was
122 determined in the presence or absence of 1 μM nocodazole in 96-well plates (Fig. S1).
123 The results show that nocodazole has a transfection-enhancing activity at 1 μM, similar
124 to colchicine (Fig. S1).
125 We further examined whether microtubule inhibitors are effective against
126 various transfection reagents with different mechanisms. Effectene (a non-liposomal
127 lipid reagent) and Viofectin (a non-lipid high-charge cationic polymer reagent) were
128 examined in addition to the previously used Lipofectamine 2000 (a cationic lipid
129 reagent). In the presence of 300 nM colchicine, the transfection efficiencies in all these
130 transfection reagents increased, although the degree of effectiveness varied (Fig. S2).
131 The increase in transfection efficiency in the presence of 300 nM colchicine was
132 approximately 2-, 6-, and 29-fold in Effectene, Viofectin, and Lipofectamine 2000,
133 respectively (Fig. S2), suggesting that colchicine is effective with various non-viral
134 transfection reagents.
135
136 **Microtubule inhibitors enhance gene transfection efficiency**
137 To further evaluate the effects of microtubule inhibitors on DNA transfection efficiency,
138 we selected two commonly used microtubule inhibitors, colchicine and vinblastine.
139 These were ranked second and third, respectively, in the 2nd screening (Fig. 2A). First,
140 we examined the dose-dependency of these inhibitors in MEF cells (Fig. 2C). Cells
141 were treated with colchicine or vinblastine at various concentrations and transfected
142 with the pCMV-Luc DNA plasmid. Then, their luciferase activity was measured to

143 determine transfection efficiency. Transfection efficiency increased in a dose-dependent
144 manner in the MEF cells (Fig. 2C). Statistical analysis showed that the EC50 (half-
145 maximal effective concentration) of colchicine and vinblastine was 239.1 and 26.29 nM,
146 respectively, in the MEF cells (Fig. 2C). Furthermore, we evaluated transfection
147 efficiency by observing GFP expression in MEF cells. The number of GFP-positive
148 cells was greater in colchicine- and vinblastine-treated cells than in DMSO-treated
149 control cells, and cell viability was approximately 70% in both drug-treated cells
150 compared with that in the control under these conditions (Fig. 2D). These results
151 suggest that treatment with colchicine and vinblastine can enhance transfection
152 efficiency.

153 As microtubule depolymerization activates the transcription factor NF-κB to
154 induce NF-κB-dependent gene expression (Rosette & Karin, 1995) and the CMV
155 promoter in the pCMV-Luc plasmid possesses an NF-κB binding site (Rosette & Karin,
156 1995; Wang & MacDonald, 2004), treatment with microtubule inhibitors may induce
157 luciferase gene expression through NF-κB-mediated CMV promoter activation. To
158 eliminate this possibility, we tested promoter activity in a cell line (MEF-LUC cells)
159 with a CMV-driven luciferase plasmid integrated into the genome. In these cells, we
160 measured the levels of luciferase activity in the presence or absence of colchicine or
161 vinblastine. Treatment with colchicine for 27 h increased luciferase gene expression
162 only marginally (approximately 1.2-fold), which did not explain the considerably
163 greater increase (approximately 40-fold) in the transfected DNA plasmids (Fig. S3A;
164 compare with Fig. 2C). Treatment with vinblastine also yielded a similar result, with
165 almost no increase in luciferase expression (Fig. S3B; compare with Fig. 2C). These

166 results indicate that the increase in transfection efficiency in the presence of microtubule
167 inhibitors does not reflect NF-κB-dependent promoter activation.
168
169 **Transfection enhancement occurs in the presence of autophagy receptor p62**
170 As p62 acts as an inhibitory factor for DNA transfection by recruiting LC3
171 (microtubule-associated protein 1A/1B-light chain 3; also called ATG8), a marker
172 protein for autophagosomes, to transfected DNA (Tsuchiya *et al.* 2016), the
173 transfection-enhancing activity of the tested compounds may be deduced by the
174 invalidation of the p62-dependent autophagic pathway. Based on this hypothesis, we
175 examined the activity of the 87 compounds at a concentration of 1 μM in p62KO-MEF
176 cells under the same conditions as those in Fig. 2A (Fig. 3A). All compounds exhibited
177 little or no transfection-enhancing activity in p62KO-MEF cells (Fig. 3A). As the
178 microtubule inhibitors (compounds 1–9 in Fig. 2B) seemed to show a slight increase in
179 transfection enhancing activity (Fig. 3A), we further tested colchicine and vinblastine
180 for transfection-enhancing activity at various concentrations from 15.6 to 2000 nM (Fig.
181 3B, C) and found that these two microtubule inhibitors did not show transfection-
182 enhancing activity at any of the tested concentrations (Fig. 3B, C). This result suggests
183 that microtubule inhibitors function in a p62-dependent autophagic pathway.
184
185 **p62-dependent ubiquitination is delayed by microtubule inhibitors**
186 To understand the molecular mechanisms of the p62-dependent enhancement of
187 transfection efficiency by colchicine and vinblastine, we employed an experimental
188 method using polystyrene beads that had been developed to monitor the behavior of the
189 transfected DNA (Kobayashi *et al.* 2010) (Fig. 4A). In this method, the beads are

190 incorporated into cells with transfection reagents via endocytosis and enter the cytosol
191 after rupture of the endosomal membrane. The beads that appeared in the cytosol were
192 targeted for autophagy, similar to the transfected DNA (Kobayashi *et al.* 2010;
193 Kobayashi *et al.* 2015) (Fig. 4A). For monitoring in living cells, the beads were pre-
194 conjugated with pHrodo dye, which emits fluorescence under acidic pH conditions,
195 such as those in the acidic endosome but not in the cytosol. Therefore, this dye serves as
196 a marker of endosome membrane rupture, as previously described (Kobayashi *et al.*
197 2010). The pHrodo-conjugated beads were incorporated into MEF cells expressing
198 GFP-fused Ub protein (GFP-Ub MEF cells) (Tsuchiya *et al.* 2018), and the assembly of
199 GFP-Ub around the beads was observed in a living cell using time-lapse fluorescence
200 microscopy (Fig. 4B). In the control DMSO-treated cells, the time for Ub recruitment to
201 the beads was approximately 3–4 min (Fig. 4B, middle panel) after the disappearance of
202 pHrodo fluorescence (Fig. 4B, upper panel). In contrast, the time for GFP-signal
203 accumulation was 9–10 min in 500 nM colchicine-treated MEF cells (Fig. 4C, middle
204 panel), which was longer than that in the control cells (Fig. 4B). Statistical analysis was
205 performed to determine the timing of GFP-signal accumulation around the beads after
206 the loss of pHrodo signals in cells expressing GFP-Ub with or without the inhibitor
207 (Fig. 4D). In the DMSO-treated cells, the time for Ub recruitment to the beads was ~4
208 min (median) after the disappearance of pHrodo fluorescence (mean and SD, 4.167 ±
209 1.88 min, n = 24 beads; lane 1 in Fig. 4D). Moreover, the timing of GFP-signal
210 accumulation was ~6 min (median) in the 100 nM colchicine-treated MEF cells (mean
211 and SD: 8.286 ± 8.36 min, n = 28 beads: lane 2 in Fig. 4D), ~11 min (median) in the
212 500 nM colchicine-treated MEF cells (mean and SD: 11.32 ± 11.30 min, n = 22 beads:
213 lane 3 in Fig. 4D), and ~6 min (median) in the vinblastine-treated MEF cells (mean and

214 SD: 6.48 ± 3.81 min, *n* = 31 beads; lane 4 in Fig. 4D). Additionally, the GFP-Ub signals
215 did not accumulate within 60 min in colchicine- or vinblastine-treated GFP-Ub MEF
216 cells (these beads were not counted and were not included in the *n*; upper column in Fig.
217 4D). These results show that GFP-Ub accumulation around the beads was significantly
218 delayed in colchicine- or vinblastine-treated MEF cells. Colchicine and vinblastine have
219 different effects on microtubule depolymerization; colchicine forms diffusely
220 distributed tubulins/microtubules, whereas vinblastine forms the paracrystal structure of
221 the microtubules (Haraguchi *et al.* 1997). Nonetheless, both have the same function of
222 increasing DNA transfection efficiency, suggesting that normal microtubule function or
223 structure is important for Ub recruitment to the target site.
224
225 **Active form of p62 is suppressed by microtubule inhibitors**
226 It has been reported that the phosphorylated form of p62 at amino acid residue S405
227 (p62 S405) is required for Ub recruitment during selective autophagy (Tsuchiya *et al.*
228 2018). Therefore, Ub recruitment can be delayed by a decrease in the level of
229 phosphorylated p62 at S405. To test this hypothesis, we performed Western blot
230 analysis to evaluate the total p62 protein levels and p62 S405 phosphorylation levels
231 (Fig. 5). The p62 S405 phosphorylation levels were very low before DNA transfection
232 ("no transfection" in Fig. 5). However, after transfection ("DNA transfection 24 h"),
233 these levels greatly increased in DMSO-treated MEF cells, although the p62 levels
234 remained unchanged. This suggests that DNA transfection induced an increase in p62
235 S405 phosphorylation. However, in MEF cells treated with colchicine or vinblastine,
236 the level of p62 S405 phosphorylation decreased. This suggests that microtubule
237 inhibitors inhibit Ub recruitment by decreasing the level of phosphorylated p62 at S405.

238

239 **Discussion**

240 **Microtubule structure/function and transfection efficiency**

241 In this study, we used a non-biased, high-throughput screening approach to identify
242 small chemical compounds that increase DNA transfection efficiency and identified
243 microtubule inhibitors as the top 9 compounds. Therefore, inhibition of the microtubule
244 structure or function seems to trigger an increase in transfection efficiency. This finding
245 is consistent with previous reports that microtubule depolymerizing reagents,
246 nocodazole, increased transfection efficiency in CV-1 cells (Lindberg *et al.* 2001) and
247 colchicine and vinblastine increased transfection efficiency in cultured vascular smooth
248 muscle cells (Wang & MacDonald 2004). Additionally, microtubule-polymerizing
249 reagents, such as paclitaxel, also increase the transfection efficiency in COS-7 and A549
250 cells (Hasegawa *et al.* 2001; Nair *et al.* 2002). The polymerizing agent docetaxel, a
251 chemical compound closely related to paclitaxel, was included in our screening results
252 for the top 9 compounds (Fig. 2B, Rank 7). Moreover, tubulin deacetylation inhibitors,
253 such as HDAC6 inhibitors, also increase transfection efficiency in A549 cells, PC3
254 cells, and mesenchymal stem cells (Vaughan *et al.* 2008; Barua & Rege 2010; Ho *et al.*
255 2017). This is likely because acetylated tubulin can stabilize microtubule structures,
256 which in turn implies that microtubule structure stabilization can also increase gene
257 transfection efficiency. Taken together, these findings strongly suggest that inhibition of
258 the intact structure or dynamic nature of microtubules is important for increasing the
259 efficiency of gene transfection.

260

261 **Microtubule inhibitors affect selective autophagy pathways**

262 Our results showed that treatment of cells with colchicine or vinblastine increased
263 transfection efficiency in a p62-dependent manner. However, it is difficult to attribute
264 these observations to a particular cause. Microtubules are major contributors to the
265 trafficking of several components in the endosomal/lysosomal pathway; hence, it is
266 logical to propose that these inhibitors may block the autophagy pathway. The role of
267 microtubules in autophagosome formation appears to be different based on the culture
268 medium conditions, e.g., vegetatively growing medium (basal) or starvation medium
269 (inducible) conditions. Several studies have used microtubule inhibitors under basal
270 conditions to show that microtubules do not participate in autophagosome formation
271 (Reunanen *et al.* 1988; Aplin *et al.* 1992; Kochl *et al.* 2006). However, under inducible
272 conditions, disassembling the microtubules with these inhibitors prevented
273 autophagosome formation, suggesting that microtubules play a crucial role in this
274 process (Kochl *et al.* 2006; Geeraert *et al.* 2010). Previous studies have shown that
275 transfected DNA also induces the selective autophagy pathway (Roberts *et al.* 2013;
276 Chen *et al.* 2014; Tsuchiya *et al.* 2016); hence, microtubule inhibitors may affect
277 transfection-induced autophagosome formation. The detailed mechanisms of the
278 inhibition of autophagosome formation following microtubule inhibitor treatment are
279 not clear; however, several autophagy factors are associated with microtubules,
280 including ATG8 (LC3), ATG1 (ULK1), ATG6 (Beclin1), ATG18 (WIPI1), and p62
281 (Mackeh *et al.* 2013). LC3 has long been thought to be involved in the regulation of
282 microtubule assembly and disassembly (Mann & Hammarback 1994; Deretic 2008).
283 Furthermore, ATG18-positive pre-autophagosomal structures can move along
284 microtubules, and this movement is extremely sensitive to microtubule inhibitor
285 treatment (Polson *et al.* 2010). These data suggest that microtubules contribute to the

286 sequestration, recruitment, and movement of autophagy factors for the formation of
287 inducible autophagosomes. Therefore, microtubule inhibitors may block the inducible
288 autophagy pathway, resulting in a decrease in the likelihood of DNA degradation and
289 increase in transfection efficiency.
290
291 **Microtubule inhibitors decrease the level of phosphorylated p62**
292 The ubiquitination of endosome membrane proteins surrounding exogenous material,
293 such as transfected DNA, is the initial step in inducible selective autophagy (Randow
294 2011; Wileman 2013; Tsuchiya *et al.* 2016). In our study, treatment with colchicine or
295 vinblastine delayed the recruitment of Ub proteins. This delay in recruitment is also
296 caused by the depletion of p62 or mutation of the p62 phosphorylation site at S405
297 (human S403) (Tsuchiya *et al.* 2018). As p62 has been reported as a microtubule-
298 associated factor (Geeraert *et al.* 2010), treatment with a microtubule inhibitor may
299 affect p62-mediated Ub recruitment. Specifically, our results showed that p62 S405
300 phosphorylation was significantly impaired by treatment with colchicine or vinblastine
301 after transfection. p62 S405 is phosphorylated by kinases such as CK2 and TBK1
302 (Matsumoto *et al.* 2011; Matsumoto *et al.* 2015). These kinases are also associated with
303 tubulin (Faust *et al.* 1999; Lim *et al.* 2004; Pillai *et al.* 2015; Yang *et al.* 2018). After
304 transfection, the recruitment of these kinases may be affected by treatment with
305 microtubule inhibitors. Further studies are necessary to elucidate the detailed
306 mechanisms by which these microtubule inhibitors affect the phosphorylation levels of
307 p62.
308 In this study, a non-biased high-throughput screening method revealed that
309 microtubule inhibitors are the most effective reagents for increasing transfection

310 efficiency among the drugs present in the Osaka University compound library, and
311 revealed for the first time, the mechanism by which microtubule inhibitors increase
312 transfection efficiency; that is, microtubule inhibitors suppress p62 phosphorylation,
313 which is required for autophagosome formation to degrade transfected DNA. Our
314 findings provide solutions to increase transfection efficiency.
315

316 **Experimental procedures**

317 **Plasmids**

318 pCMV-Luc plasmid encoding the luciferase gene *luc2*, used as a luciferase expression
319 vector in this study, was purchased from Promega (E1310; pGL4.50 [*luc2*/CMV/Hygro]
320 vector; Promega, Madison, WI, USA). The GFP expression plasmid pCMX-AFAP was
321 prepared as previously described (Ogawa *et al.* 2004).

322 To create cells stably expressing luciferase (see the next section), we constructed
323 the PB-CMV-LUC-Zeo vector. We first constructed the PB-EF1-MCS-IRES-Zeo
324 vector. To insert the zeocin resistance gene DNA sequence, two DNA fragments (#1
325 and #2) were amplified as follows: the cloning site with Kozak sequence fragment #1
326 was amplified from the PB-EF1-MCS-IRES-Neo vector (PB533A-2; System
327 Biosciences, Palo Alto, CA, USA) using PCR and the following primers: 5′-
328 CTGAAGGATGCCCAGAAGGTACCCCATTGT-3′ and 5′-
329 TCCGGACGCCATGGTTGTGG-3′. The zeocin coding fragment #2 was amplified
330 from the pcDNA3.1/Zeo (+) vector (V86020; Thermo Fisher Scientific, Yokohama,
331 Japan) using PCR and the following primers: 5′-
332 ACAACCATGGCGTCCGGAATGGCCAAGTTGACCAGTGCCGTTCC-3′ and 5′-
333 TCCAGAGGTTGATTGTCGACTCAGTCCTGCTCCTCGGCCACGAA-3′.

334 Following digestion with KpnI and SalI, fragments #1 and #2 were inserted into the PB-
335 EF1-MCS-IRES-Neo vector using the In-Fusion HD Cloning Kit (639648; Takara Bio
336 Inc. Kusatsu, Japan). This resulted in the PB-EF1-MCS-IRES-Zeo vector. Next, the
337 human cytomegalovirus immediate early enhancer and promoter (CMV-IE) DNA
338 sequence (#3) was amplified from the pGL4.50 [*luc2*/CMV/Hygro] vector using PCR
339 and the following primers: 5′-
340 GGGGATACGGGGAAAAGGCCTCGTTACATAACTTACGGTAAATG-3′ and 5′-
341 GAATTCGCTAGCTCTAGAAGCTCTGCTTATATAGACCTCCCACC-3′. The
342 luciferase DNA sequence (#4) was amplified from the pGL4.50 [*luc2*/CMV/Hygro]
343 vector using PCR and the following primers: 5′-
344 TCTAGAGCTAGCGAATTCATGGAAGATGCCAAAAACATTAAGAA-3′ and 5′-
345 CGATTTAAATTCGAATTCTTACACGGCGATCTTGCCGCCCTTCT-3′. Following
346 digestion with EcoRI and StuI, fragments #3 and #4 were inserted into the PB-EF1-
347 MCS-IRES-Zeo vector using the In-Fusion HD Cloning Kit. This resulted in the PB-
348 CMV-LUC-Zeo vector.
349
350 **Cell strains**
351 p62KO-MEF cells (p62$^{-/-}$ cells) and their parental MEF cells were kindly provided by
352 Dr. Tetsuro Ishii (University of Tsukuba) (Komatsu *et al.* 2007). MEF cells stably
353 expressing GFP-Ub were generated as previously described (Tsuchiya *et al.* 2018). To
354 obtain MEF cells or p62KO-MEF cells stably expressing luciferase, MEF cells or
355 p62KO-MEF cells were transfected with the PB-CMV-LUC-Zeo plasmid (generated as
356 described in the previous section) and cultured in the presence of 100 μg/mL Zeocin
357 (R25501, Thermo Fisher Scientific), and then, single clones (MEF-LUC cells) were

358 selected. Each stable clone was examined for luciferase protein expression using a
359 luciferase assay.
360
361 **Cell culture**
362 All cell lines were maintained in culture medium (Dulbecco's modified Eagle medium
363 (DMEM) (D6429; Sigma-Aldrich, St. Louis, MO, USA) supplemented with 10% fetal
364 bovine serum) in the presence of 5% CO_2 at 37°C.
365
366 **High-throughput screening for enhancer compounds**
367 The MEF cells were seeded at a density of 0.8×10^3 cells per well (384-well microplate,
368 781091; Greiner Bio-One, Tokyo, Japan) using a Multidrop COMBI (Thermo Fisher
369 Scientific) and cultured for 6 h in culture medium. The cells were pretreated for 18 h
370 with 1% DMSO (negative control) or the screening compounds (10 μM each) using a
371 Fluent780® Automation Workstation (Tecan Japan, Kawasaki, Japan) with a 96-
372 channel head adapter and Tecan sterile tips (30048824; Tecan Japan). The pretreated
373 cells in each well were transfected with 25 ng of pCMV-Luc plasmid using
374 Lipofectamine 2000 (Thermo Fisher Scientific) for 28 h in the presence of each
375 compound. Cell viability was measured with the RealTime-Glo™ MT Cell Viability
376 Assay (E9713; Promega) using the GloMax® Discover Microplate Reader (Promega).
377 Luciferase activity was measured with the ONE-Glo™ Luciferase Assay System
378 (E6120; Promega) using the GloMax® Discover Microplate Reader according to the
379 manufacturer's protocol. The values of luciferase activity were normalized to the cell
380 number obtained from cell viability measurements.
381

382 **Transfection efficiency measurements**

383 Transfection efficiency was determined based on the luciferase activity expressed from
384 the transfected plasmid. Cells were seeded at a density of 0.45×10^4 cells per well (96-
385 well assay plate; 3603 Corning, Corning, NY, USA) and cultured overnight in culture
386 medium. The cells were pretreated with 1% DMSO (negative control) or the screening
387 compounds (0.1–10 μM each) for 30 min. The cells were then transfected with 100 ng
388 of pCMV-Luc plasmid using Lipofectamine 2000 for 28 h in the presence of each
389 compound. Cell viability was measured with the RealTime-Glo™ MT Cell Viability
390 Assay using the GloMax® 96 Microplate Luminometer (Promega). Luciferase activity
391 was measured with the ONE-Glo™ Luciferase Assay System using the GloMax® 96
392 Microplate Luminometer according to the manufacturer's protocol. The values of
393 luciferase activity were normalized to the cell number obtained from cell viability
394 measurements. Mean EC50 values and SDs were determined from three independent
395 experiments. Transfection efficiencies were determined by luciferase activity
396 normalized to cell viability.

397 Viofectin (VFT1001; Viogene, Nacalai tesque, Kyoto, Japan) and Effectene
398 (301425; Qiagen, Tokyo, Japan) were also used as transfection reagents. For Viofectin,
399 the same transfection procedure as that described above for Lipofectamine 2000 was
400 used, except that the reagents were different. For Effectene, some procedures were
401 modified as follows: initial cell density was 1×10^4 cells per well and the cells were
402 transfected for 4 h and further incubated for another 20 h in culture medium without
403 transfection reagents.

404

405 **GFP expression**

406 MEF cells were seeded at a density of 1.5×10^5 cells per well (6-well assay plate; 3335
407 Corning, Corning, NY, USA) and cultured overnight in culture medium. The cells were
408 pretreated with 1% DMSO (negative control), 250 nM cholchicine, or 50 nM
409 vinblastine for 30 min. The cells were then transfected with 2 μg of pCMV-Luc plasmid
410 using Lipofectamine 2000 for 24 h in the presence of each drug. The cells were
411 observed using an objective lens (N Plan 5x/0.12 PH 0) on a Leica DM IL LED
412 fluorescence microscope (Leica Microsystems, Wetzlar, Germany).
413
414 **Preparation of pHrodo-conjugated beads**
415 pHrodo-conjugated beads were prepared as previously described (Kobayashi *et al.*
416 2010). Briefly, Dynabeads M-270 Streptavidin (DB65306; Thermo Fisher Scientific)
417 were washed three times with phosphate buffered saline (PBS) and resuspended in 100
418 mM sodium bicarbonate buffer (pH 8.5) to an appropriate concentration (typically a
419 1:10 or 1:20 dilution). pHrodo-succinimidyl ester (P36600; Thermo Fisher Scientific)
420 was then added to the bead suspension and incubated in sodium bicarbonate buffer for 1
421 h at room temperature (about 26°C). After the conjugation reaction, the beads were
422 washed with sodium bicarbonate buffer and suspended in PBS.
423
424 **Incorporation of beads into living cells**
425 One day before incorporating the beads, GFP-Ub MEF cells were seeded onto 35 mm
426 glass-bottom culture dishes (P35G-1.5-10-C; MatTek, Ashland, MA, USA) at a density
427 of 1.5×10^5 cells/dish in culture medium. The cells were pretreated with each
428 microtubule inhibitor (100 nM colchicine, 500 nM colchicine, or 100 nM vinblastine) or
429 DMSO as a control for 30 min at 37°C in a CO_2 incubator before bead incorporation.

430 The transfection reagent Effectene (301425; Qiagen, Tokyo, Japan) was used to
431 incorporate the beads. Transfection-reagent-coated beads were prepared by mixing
432 pHrodo-conjugated beads with the Effectene transfection reagent according to the
433 manufacturer's protocol, except that a bead suspension was used instead of the DNA
434 solution. The resulting bead mixture (~10 μL) was mixed with 90 μL of the culture
435 medium containing each microtubule inhibitor and added to the cells by replacing the
436 medium. After incubation for 1 h at 37°C in a CO_2 incubator, the cells were washed
437 twice with fresh growth medium to remove unattached beads and then further incubated
438 with the medium containing each microtubule inhibitor or control DMSO for the time
439 indicated in each experiment.
440
441 **Time-lapse imaging**
442 Cells were treated with 100 ng/mL Hoechst 33342 (B2261; Sigma-Aldrich) for 15 min
443 to stain chromosomes, as previously described (Haraguchi *et al.* 1997), except that the
444 medium containing each microtubule inhibitor or control DMSO was used. After
445 washing with the culture medium, the cells were cultured in fresh culture medium
446 (phenol red-free DMEM containing 10% fetal bovine serum) containing each
447 microtubule inhibitor or control DMSO. Time-lapse observations were performed using
448 an oil-immersion objective lens (UApo40/NA1.35; Olympus, Tokyo, Japan) on a
449 DeltaVision microscope system (GE Healthcare Life Sciences Japan, Tokyo, Japan)
450 placed in a temperature-controlled room (37°C), as previously described (Haraguchi *et*
451 *al.* 1997). Images were obtained every minute for approximately 60 min.
452 The timing of GFP-Ub fluorescence signal accumulation around the beads was
453 determined as previously described (Tsuchiya *et al.* 2018). Briefly, the fluorescence

454 intensity of the region (18 pixels square) surrounding the beads was measured using the
455 FUJI software suite (IMAGE J; National Institutes of Health, Bethesda, MD, USA), and
456 the background fluorescence intensity of the region with no beads in the same cell was
457 subtracted.
458
459 **Western blot analysis**
460 MEF cells were seeded at a density of 1.5×10^5 cells per well (6-well assay plate; 3335
461 Corning, Corning, NY, USA) and cultured overnight in culture medium. The cells were
462 pretreated with 1% DMSO (negative control), 500 nM colchicine, or 100 nM
463 vinblastine for 30 min. The cells were then transfected with 2 μg of pCMX-AFAP
464 plasmid using Lipofectamine 2000 for 24 h in the presence of each drug. Western blot
465 analysis was performed as previously described (Tsuchiya *et al.* 2018). Briefly, cell
466 lysates were prepared in a lysis buffer [50 mM Tris-HCl, pH 7.5, 150 mM NaCl, 1 mM
467 EDTA, 1% Triton X-100, 1 x Phosphatase Inhibitor Cocktail Solution Ⅱ (160-24371;
468 FUJIFILM Wako Pure Chemical Corporation, Osaka, Japan) and 1 x protease inhibitor
469 cocktail (Nacalai tesque Inc., Kyoto, Japan)]. The lysates were subjected to
470 electrophoresis on NuPAGE 4% to 12% Bis-Tris gels (NP0321; Thermo Fisher
471 Scientific). Proteins were transferred to polyvinylidene fluoride membranes and probed
472 using anti-p62 (SQSTM1) (PM045; MBL, Nagoya, Japan), anti-Phospho-
473 SQSTM1/p62(Ser403) (D8D6T; Cell Signaling Technology, Danvers, MA, USA), and
474 anti-glyceraldehyde 3-phosphate dehydrogenase (GAPDH) (14C10; Cell Signaling
475 Technology) antibodies, and secondary antibody conjugated to horseradish peroxidase
476 (NA9340V; GE Healthcare Life Sciences). Protein bands were stained with

477 ImmunoStar Zeta (295-72404; FUJIFILM Wako Pure Chemical Corporation) and
478 detected by chemiluminescence using a ChemiDoc MP imaging system (Bio-Rad,
479 Tokyo, Japan).
480
481 **Statistical analysis**
482 The *p*-values were obtained by performing Kruskal-Wallis tests using GraphPad Prism
483 8 software (GraphPad Software, Inc., La Jolla, CA, USA).

484

485 **Acknowledgments**
486 This work is dedicated to the late Professor Tomoko Ogawa. We are grateful to Dr. Eiji
487 Warabi and Dr. Tetsuro Ishii (Tsukuba University) for providing p62KO-MEF cells and
488 the corresponding wild-type MEF cells. We thank J. Iacona, Ph.D., from Edanz Group
489 (https://en-author-services.edanzgroup.com/ac) for English-editing a draft of this
490 manuscript. This study was supported by The JSPS Kakenhi Grant Numbers
491 JP19K06488 to MT, JP19KK0218, JP20H05322 and JP20K07029 to HO, JP18H05533
492 and JP20H00454 to YH, and JP17K19505 and JP18H05528 to TH. This research was
493 supported by Platform Project for Supporting Drug Discovery and Life Science
494 Research (Basis for Supporting Innovative Drug Discovery and Life Science Research
495 (BINDS)) from AMED under Grant Number JP20am0101084.
496

497 **Author contributions**

MT, HO, KW, TK, CM, KN, BL and AT performed the experiments. MT, HO, AT, YH, and TH designed the experiments. All authors analyzed and discussed the data, and MT, HO, YH, and TH wrote the manuscript.

Conflict of interest

All authors declare that: (i) no support, financial or otherwise, has been received from any organization that may have an interest in the submitted work; and (ii) there are no other relationships or activities that could appear to have influenced the submitted work.

506 **References**

507 Alomairi, J., Bonacci, T., Ghigo, E. & Soubeyran, P. (2015) Alterations of host cell
508 ubiquitination machinery by pathogenic bacteria. *Frontiers in cellular and*
509 *infection microbiology* **5**, 17. https://doi.org/10.3389/fcimb.2015.00017
510 Aplin, A., Jasionowski, T., Tuttle, D.L., Lenk, S.E. & Dunn, W.A., Jr. (1992)
511 Cytoskeletal elements are required for the formation and maturation of autophagic
512 vacuoles. *J Cell Physiol* **152**, 458-466. https://doi.org/10.1002/jcp.1041520304
513 Barua, S. & Rege, K. (2010) The influence of mediators of intracellular trafficking on
514 transgene expression efficacy of polymer-plasmid DNA complexes. *Biomaterials*
515 **31**, 5894-5902. https://doi.org/10.1016/j.biomaterials.2010.04.007
516 Chen, X., Khambu, B., Zhang, H., Gao, W., Li, M., Chen, X., Yoshimori, T. & Yin,
517 X.M. (2014) Autophagy induced by calcium phosphate precipitates targets
518 damaged endosomes. *Journal of Biological Chemistry* **289**, 11162-11174.
519 https://doi.org/10.1074/jbc.m113.531855
520 Deretic, V. (2008) Autophagosome and phagosome. *Methods Mol Biol* **445**, 1-10.
521 https://doi.org/10.1007/978-1-59745-157-4_1
522 Dupont, N., Temime-Smaali, N. & Lafont, F. (2010) How ubiquitination and autophagy
523 participate in the regulation of the cell response to bacterial infection. *Biology of*
524 *the Cell* **102**, 621-634. https://doi.org/10.1042/BC20100101
525 Faust, M., Schuster, N. & Montenarh, M. (1999) Specific binding of protein kinase CK2
526 catalytic subunits to tubulin. *FEBS letters* **462**, 51-56.
527 https://doi.org/10.1016/S0014-5793(99)01492-1
528 Galluzzi, L., Baehrecke, E.H., Ballabio, A. *et al.* (2017) Molecular definitions of
529 autophagy and related processes. *The EMBO journal* **36**, 1811-1836.
530 https://doi.org/10.15252/embj.201796697
531 Geeraert, C., Ratier, A., Pfisterer, S.G., Perdiz, D., Cantaloube, I., Rouault, A.,
532 Pattingre, S., Proikas-Cezanne, T., Codogno, P. & Pous, C. (2010) Starvation-
533 induced hyperacetylation of tubulin is required for the stimulation of autophagy by
534 nutrient deprivation. *J Biol Chem* **285**, 24184-24194.
535 https://doi.org/10.1074/jbc.M109.091553

536 Haraguchi, T., Kaneda, T. & Hiraoka, Y. (1997) Dynamics of chromosomes and
537 microtubules visualized by multiple-wavelength fluorescence imaging in living
538 mammalian cells: effects of mitotic inhibitors on cell cycle progression. *Genes to*
539 *Cells* **2**, 369-380. https://doi.org/10.1046/j.1365-2443.1997.1280326.x
540 Hasegawa, S., Hirashima, N. & Nakanishi, M. (2001) Microtubule involvement in the
541 intracellular dynamics for gene transfection mediated by cationic liposomes. *Gene*
542 *Ther* **8**, 1669-1673. https://doi.org/10.1038/sj.gt.3301573.
543 Ho, Y.K., Zhou, L.H., Tam, K.C. & Too, H.P. (2017) Enhanced non-viral gene delivery
544 by coordinated endosomal release and inhibition of beta-tubulin deactylase.
545 *Nucleic Acids Research* **45**, e38. https://doi.org/10.1093/nar/gkw1143
546 Khalil, I.A., Kogure, K., Akita, H. & Harashima, H. (2006) Uptake pathways and
547 subsequent intracellular trafficking in nonviral gene delivery. *Pharmacol Rev* **58**,
548 32-45. https://doi.org/10.1124/pr.58.1.8
549 Kobayashi, S., Kojidani, T., Osakada, H., Yamamoto, A., Yoshimori, T., Hiraoka, Y. &
550 Haraguchi, T. (2010) Artificial induction of autophagy around polystyrene beads in
551 nonphagocytic cells. *Autophagy* **6**, 36-45. https://doi.org/10.4161/auto.6.1.10324
552 Kobayashi, S., Koujin, T., Kojidani, T., Osakada, H., Mori, C., Hiraoka, Y. &
553 Haraguchi, T. (2015) BAF is a cytosolic DNA sensor that leads to exogenous DNA
554 avoiding autophagy. *Proceedings of the National Academy of Sciences of the*
555 *United States of America* **112**, 7027-7032.
556 https://doi.org/10.1073/pnas.1501235112
557 Kochl, R., Hu, X.W., Chan, E.Y. & Tooze, S.A. (2006) Microtubules facilitate
558 autophagosome formation and fusion of autophagosomes with endosomes. *Traffic*
559 *(Copenhagen, Denmark)* **7**, 129-145. https://doi.org/10.1111/j.1600-
560 0854.2005.00368.x
561 Komatsu, M., Waguri, S., Koike, M. *et al.* (2007) Homeostatic levels of p62 control
562 cytoplasmic inclusion body formation in autophagy-deficient mice. *Cell* **131**, 1149-
563 1163. https://doi.org/10.1016/j.cell.2007.10.035
564 Lim, A.C., Tiu, S.Y., Li, Q. & Qi, R.Z. (2004) Direct regulation of microtubule
565 dynamics by protein kinase CK2. *J Biol Chem* **279**, 4433-4439.
566 https://doi.org/10.1074/jbc.M310563200

567 Lindberg, J., Fernandez, M.A., Ropp, J.D. & Hamm-Alvarez, S.F. (2001) Nocodazole
568 treatment of CV-1 cells enhances nuclear/perinuclear accumulation of lipid-DNA
569 complexes and increases gene expression. *Pharmaceutical Research* **18**, 246-249.
570 https://doi.org/10.1023/a:1011001022570
571 Mackeh, R., Perdiz, D., Lorin, S., Codogno, P. & Pous, C. (2013) Autophagy and
572 microtubules - new story, old players. *Journal of Sell Science* **126**, 1071-1080.
573 https://doi.org/10.1242/jcs.115626
574 Mann, S.S. & Hammarback, J.A. (1994) Molecular characterization of light chain 3. A
575 microtubule binding subunit of MAP1A and MAP1B. *J Biol Chem* **269**, 11492-
576 11497. https://doi.org/10.1016/S0021-9258(19)78150-2
577 Matsumoto, G., Shimogori, T., Hattori, N. & Nukina, N. (2015) TBK1 controls
578 autophagosomal engulfment of polyubiquitinated mitochondria through
579 p62/SQSTM1 phosphorylation. *Human Molecular Genetics* **24**, 4429-4442.
580 https://doi.org/10.1093/hmg/ddv179
581 Matsumoto, G., Wada, K., Okuno, M., Kurosawa, M. & Nukina, N. (2011) Serine 403
582 phosphorylation of p62/SQSTM1 regulates selective autophagic clearance of
583 ubiquitinated proteins. *Molecular Cell* **44**, 279-289.
584 https://doi.org/10.1016/j.molcel.2011.07.039
585 Midoux, P., Breuzard, G., Gomez, J.P. & Pichon, C. (2008) Polymer-based gene
586 delivery: a current review on the uptake and intracellular trafficking of polyplexes.
587 *Curr Gene Ther* **8**, 335-352. https://doi.org/10.2174/156652308786071014
588 Mizushima, N., Yoshimori, T. & Ohsumi, Y. (2011) The role of Atg proteins in
589 autophagosome formation. *Annu Rev Cell Dev Biol* **27**, 107-132.
590 https://doi.org/10.1146/annurev-cellbio-092910-154005
591 Nair, R.R., Rodgers, J.R. & Schwarz, L.A. (2002) Enhancement of transgene expression
592 by combining glucocorticoids and anti-mitotic agents during transient transfection
593 using DNA-cationic liposomes. *Mol Ther* **5**, 455-462.
594 https://doi.org/10.1006/mthe.2002.0567
595 Nakatogawa, H., Suzuki, K., Kamada, Y. & Ohsumi, Y. (2009) Dynamics and diversity
596 in autophagy mechanisms: lessons from yeast. *Nature Reviews. Molecular Cell*
597 *Biology* **10**, 458-467. https://doi.org/10.1038/nrm2708

598 Ogawa, H., Yu, R. T., Haraguchi, T., Hiraoka, Y., Nakatani, Y., Morohashi, K., &
599 Umesono, K. (2004). Nuclear structure-associated TIF2 recruits glucocorticoid
600 receptor and its target DNA. *Biochem Biophys Res Commun* **320**, 218–225.
601 https://doi.org/10.1016/j.bbrc.2004.05.161
602 Pillai, S., Nguyen, J., Johnson, J., Haura, E., Coppola, D. & Chellappan, S. (2015) Tank
603 binding kinase 1 is a centrosome-associated kinase necessary for microtubule
604 dynamics and mitosis. *Nature Communications* **6**, 10072.
605 https://doi.org/10.1038/ncomms10072
606 Polson, H.E., de Lartigue, J., Rigden, D.J., Reedijk, M., Urbe, S., Clague, M.J. &
607 Tooze, S.A. (2010) Mammalian Atg18 (WIPI2) localizes to omegasome-anchored
608 phagophores and positively regulates LC3 lipidation. *Autophagy* **6**, 506-522.
609 https://doi.org/10.4161/auto.6.4.11863
610 Randow, F. (2011) How cells deploy ubiquitin and autophagy to defend their cytosol
611 from bacterial invasion. *Autophagy* **7**, 304-309
612 https://doi.org/10.4161/auto.7.3.14539
613 Rejman, J., Bragonzi, A. & Conese, M. (2005) Role of clathrin- and caveolae-mediated
614 endocytosis in gene transfer mediated by lipo- and polyplexes. *Mol Ther* **12**, 468-
615 474. https://doi.org/10.1016/j.ymthe.2005.03.038
616 Reunanen, H., Marttinen, M. & Hirsimaki, P. (1988) Effects of griseofulvin and
617 nocodazole on the accumulation of autophagic vacuoles in Ehrlich ascites tumor
618 cells. *Exp Mol Pathol* **48**, 97-102. https://doi.org/10.1016/0014-4800(88)90048-2
619 Roberts, R., Al-Jamal, W.T., Whelband, M., Thomas, P., Jefferson, M., van den
620 Bossche, J., Powell, P.P., Kostarelos, K. & Wileman, T. (2013) Autophagy and
621 formation of tubulovesicular autophagosomes provide a barrier against nonviral
622 gene delivery. *Autophagy* **9**, 667-682. https://doi.org/10.4161/auto.23877
623 Rosette, C., & Karin, M. (1995). Cytoskeletal control of gene expression:
624 depolymerization of microtubules activates NF-kappa B. *The Journal of cell*
625 *biology*, **128**, 1111–1119. https://doi.org/10.1083/jcb.128.6.1111
626 Tachibana, K., Yuzuriha, T., Tabata, R. *et al.* (2018) Discovery of peroxisome
627 proliferator-activated receptor alpha (PPARalpha) activators with a ligand-
628 screening system using a human PPARalpha-expressing cell line. *J Biol Chem* **293**,
629 10333-10343. https://doi.org/10.1074/jbc.ra118.002077

630 Tsuchiya, M., Ogawa, H., Koujin, T., Kobayashi, S., Mori, C., Hiraoka, Y. &
631 Haraguchi, T. (2016) Depletion of autophagy receptor p62/SQSTM1 enhances the
632 efficiency of gene delivery in mammalian cells. *FEBS letters* **590**, 2671-2680.
633 https://doi.org/10.1002/1873-3468.12262
634 Tsuchiya, M., Ogawa, H., Koujin, T., Mori, C., Osakada, H., Kobayashi, S., Hiraoka, Y.
635 & Haraguchi, T. (2018) p62/SQSTM1 promotes rapid ubiquitin conjugation to
636 target proteins after endosome rupture during xenophagy. *FEBS Open Bio* **8**, 470-
637 480. https://doi.org/10.1002/2211-5463.12385
638 Vaughan, E.E., Geiger, R.C., Miller, A.M., Loh-Marley, P.L., Suzuki, T., Miyata, N. &
639 Dean, D.A. (2008) Microtubule acetylation through HDAC6 inhibition results in
640 increased transfection efficiency. *Mol Ther* **16**, 1841-1847.
641 https://doi.org/10.1038/mt.2008.190
642 Wang, L. & MacDonald, R.C. (2004) Effects of microtubule-depolymerizing agents on
643 the transfection of cultured vascular smooth muscle cells: enhanced expression
644 with free drug and especially with drug-gene lipoplexes. *Mol Ther* **9**, 729-737.
645 https://doi.org/10.1016/j.ymthe.2004.02.009
646 Wileman, T. (2013) Autophagy as a defence against intracellular pathogens. *Essays in*
647 *Biochemistry* **55**, 153-163. https://doi.org/10.1042/bse0550153
648 Yang, H., Mao, W., Rodriguez-Aguayo, C., Mangala, L.S., Bartholomeusz, G., Iles,
649 L.R., Jennings, N.B., Ahmed, A.A., Sood, A.K., Lopez-Berestein, G., Lu, Z. &
650 Bast, R.C., Jr. (2018) Paclitaxel Sensitivity of Ovarian Cancer Can be Enhanced by
651 Knocking Down Pairs of Kinases that Regulate MAP4 Phosphorylation and
652 Microtubule Stability. *Clin Cancer Res* **24**, 5072-5084.
653 https://doi.org/10.1158/1078-0432.ccr-18-0504
654

655 **Figure legends**

656 **Fig. 1. High-throughput screening for drugs enhancing transfection efficiency**

657 (A) Schematic diagram of the process of high-throughput screening using automated
658 workstations. Murine embryonic fibroblast (MEF) cells were treated with each
659 compound and then transfected with the pCMV-Luc plasmid in the presence of each
660 compound. Cell viability and the luciferase activity from the transfected plasmid were
661 measured. Transfection efficiency was evaluated based on luciferase activity normalized
662 to cell viability. (B) High-throughput screening was performed for 4,400 compounds
663 from the Osaka University compound library as described. Values of transfection
664 efficiency were plotted for the selected 4,240 compounds. Dimethyl sulfoxide (DMSO)
665 was used as the negative control. The red broken line represents the mean + 4 × SD of
666 all negative control assay points.

667

668 **Fig. 2. Second screening of compounds selected through high-throughput screening**

669 (A) The top 87 compounds identified in the primary screen were further examined.
670 MEF cells were transfected with the pCMV-Luc plasmid for 28 h in the presence of 1
671 μM of each compound. DMSO was used as the negative control. Transfection efficiency
672 was determined based on luciferase activity normalized to the cell viability. Bar graphs
673 show fold changes in transfection efficiency relative to the value from the control
674 DMSO-treated cells in descending order. The second and third columns represent data
675 for colchicine and vinblastine as indicated. (B) The top 9 potential compounds for
676 enhancement of transfection efficiency. (C) MEF cells were transfected with the

677 pCMV-Luc plasmid for 28 h in the presence of colchicine (left graph) or vinblastine
678 (right graph) at the indicated concentrations. Transfection efficiency was determined as
679 described above. Filled circles and vertical lines indicate the mean and SD, respectively,
680 of at least three independent experiments. (D) Control DMSO-treated MEF cells (a, d),
681 250 nM colchicine-treated MEF cells (b, e), and 50 nM vinblastine-treated MEF cells
682 (c, f) were examined using fluorescence microscopy 24 h after transfection with a GFP-
683 expressing plasmid pCMX-AFAP (upper panels; GFP); the lower panels represent the
684 corresponding bright-field (BF) images of the upper panels. Scale bar = 500 μm.

685

686 **Fig. 3. Colchicine- and vinblastine-treated MEF cells do not enhance transfection**
687 **efficiency in the absence of p62**

688 (A) The top 87 compounds were examined in p62KO-MEF cells. The p62KO-MEF
689 cells were transfected with the pCMV-Luc plasmid for 28 h in the presence of 1 μM of
690 each compound, and transfection efficiency was determined as described in the legend
691 to Fig. 2A. The fold changes in transfection efficiency relative to the value from the
692 control DMSO-treated cells are shown in the same order as in Fig. 2A. The two
693 columns on the right are reproduced from Fig. 2A for comparison. (B, C) The p62KO-
694 MEF cells were transfected for 28 h with the pCMV-Luc plasmid in the presence of the
695 indicated concentrations of colchicine (B) or vinblastine (C). Each value of the
696 transfection efficiency is indicated as the mean ± SD of at least three independent
697 experimental results.

698

699 **Fig 4. Colchicine- and vinblastine-treated MEF cells affect the timing of**

700 **ubiquitination**

701 (A) Schematic diagram of the experimental system using beads incorporated into cells
702 to monitor the behavior of transfected materials. (B, C) Time-lapse images of pHrodo
703 and GFP-Ub fluorescence around a single pHrodo-conjugated bead in MEF cells.
704 Images were obtained every minute for approximately 60 min. The panels show
705 representative images of pHrodo and GFP-Ub fluorescence. (B) GFP-Ub MEF cells
706 treated with DMSO as a control. Arrows indicate the timing of appearance of GFP-Ub
707 signals around the beads. (C) GFP-Ub MEF cells treated with 500 nM colchicine.
708 Arrows indicate the timing of appearance of GFP-Ub signals around the beads. Scale
709 bar = 2 μm. (D) Statistical analysis was performed for the time taken for GFP-signal
710 accumulation around the beads after the loss of pHrodo signals in the GFP-Ub MEF
711 cells. Lane 1: control treated with DMSO. Lane 2: 100 nM colchicine-treated MEF
712 cells. Lane 3: 500 nM colchicine-treated MEF cells. Lane 4: 100 nM vinblastine-treated
713 MEF cells. The median values were 4 min for GFP-Ub (n = 24 beads), 6 min for 100
714 nM colchicine (n = 28 beads), 6 min for 500 nM colchicine (n = 22 beads), and 6 min
715 for 100 nM vinblastine (n = 31 beads). Three independent experiments were performed
716 for each lane, and the total bead number is indicated as n. Statistical differences ($p <$
717 0.0001) were determined using the Kruskal–Wallis test. Error bars indicate 95%
718 confidence intervals.

719

720 **Fig. 5. Colchicine- and vinblastine-treated MEF cells decrease the level of**

721 **phosphorylated p62 at S405**

722 Western blot analysis was performed for total p62 and S405-phosphorylated p62 in
723 MEF cells. Cells were pretreated with 500 nM colchicine or 100 nM vinblastine for 30
724 min, and then transfected with the pCMX-AFAP plasmid in the presence of 500 nM
725 colchicine or 100 nM vinblastine. DMSO was used as the control. Samples were
726 subjected to Western blot analysis with no transfection or with transfection for 24 h.
727 GAPDH was used as the loading control.

728

Fig. 1

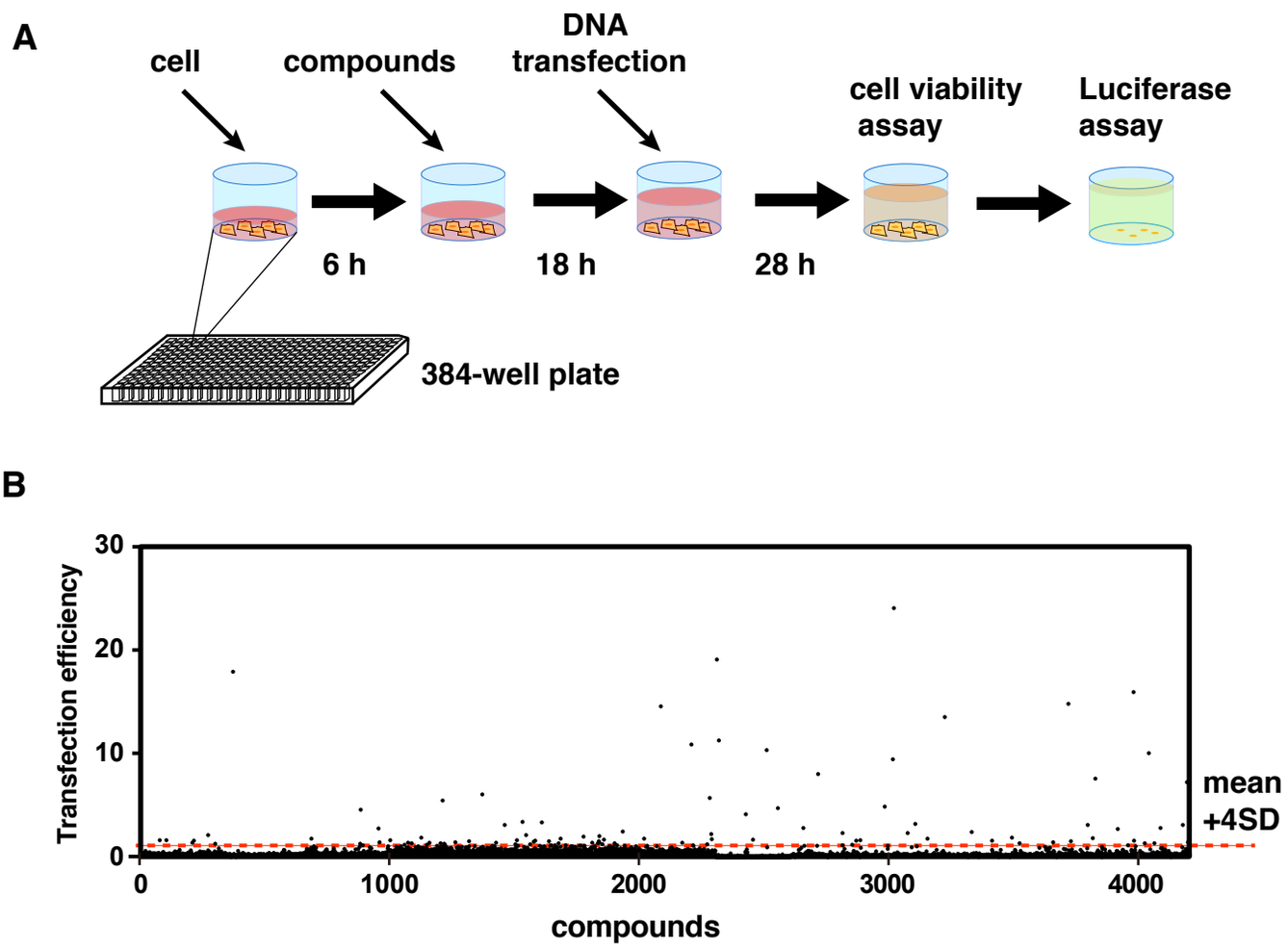
A
cell
compounds
DNA
transfection
cell viability
assay
Luciferase
assay
6 h
18 h
28 h
384-well plate
B
Transfection efficiency
30
20
10
0
0
1000
2000
3000
4000
compounds
mean
+4SD

Fig. 2

A

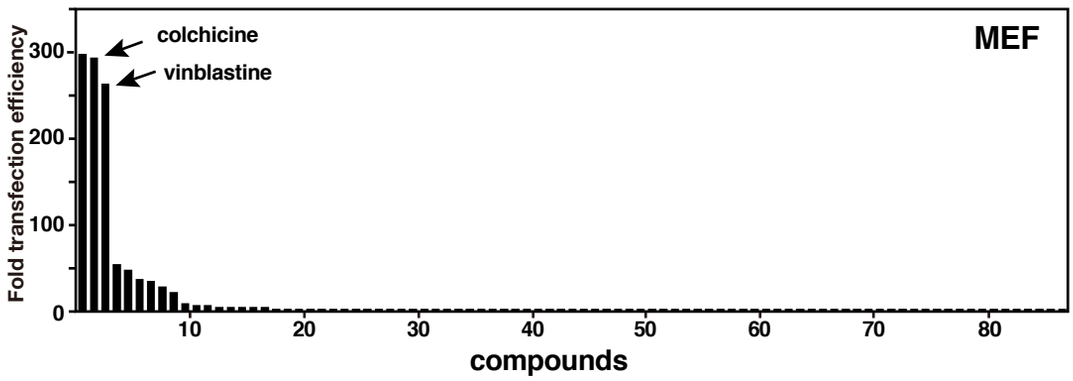

B

No	chemical name	target	function	PubChem CID
1	PODOFILOX	microtubule	antineoplastic, antimitotic agent	10607
2	COLCHICINE	microtubule	antimitotic, antigout agent	6167
3	VINBLASTINE SULFATE	microtubule	antineoplastic, spindle poison	241902
4	DEOXYSAPPANONE B 7,4'-DIMETHYL ETHER	microtubule		4026888
5	VINCRISTINE SULFATE	microtubule	antineoplastic	249332
6	PICROPODOPHYLLIN ACETATE	microtubule / IGF-1R	antineoplastic	233299
7	DOCETAXEL	microtubule	antineoplastic	148124
8	FENBENDAZOLE	microtubule	anthelmintic, antinematodal drug	3334
9	FLUBENDAZOLE	microtubule	anthelmitic, antinematodal drug	35802

C

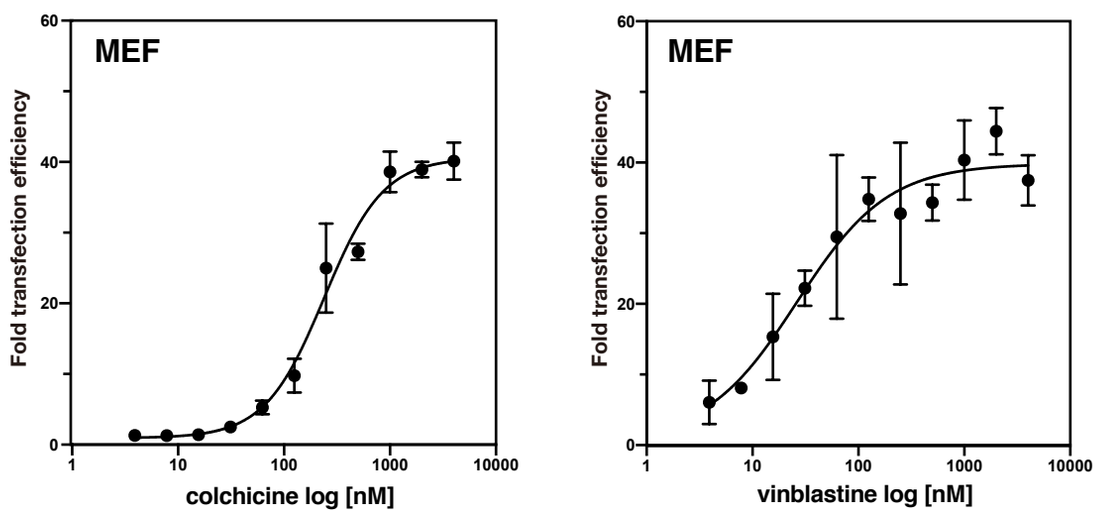

D

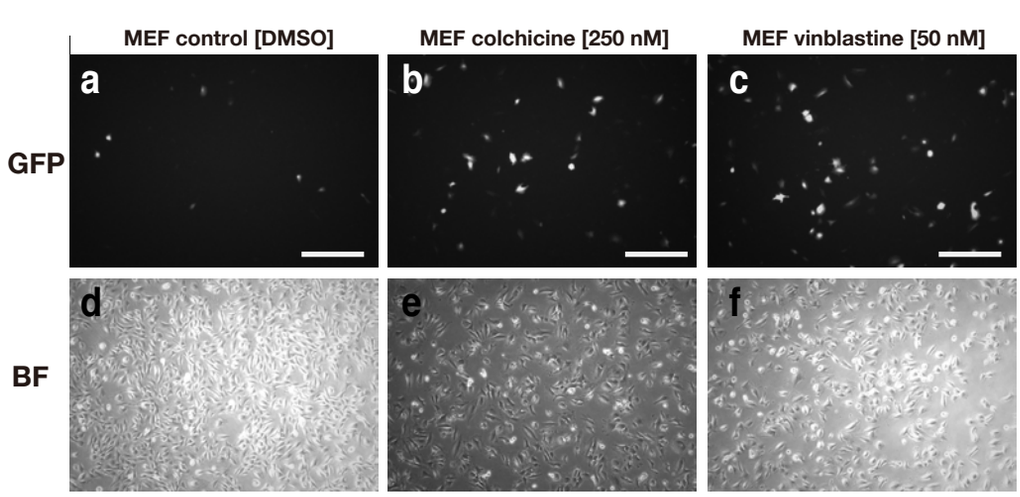

Fig. 3

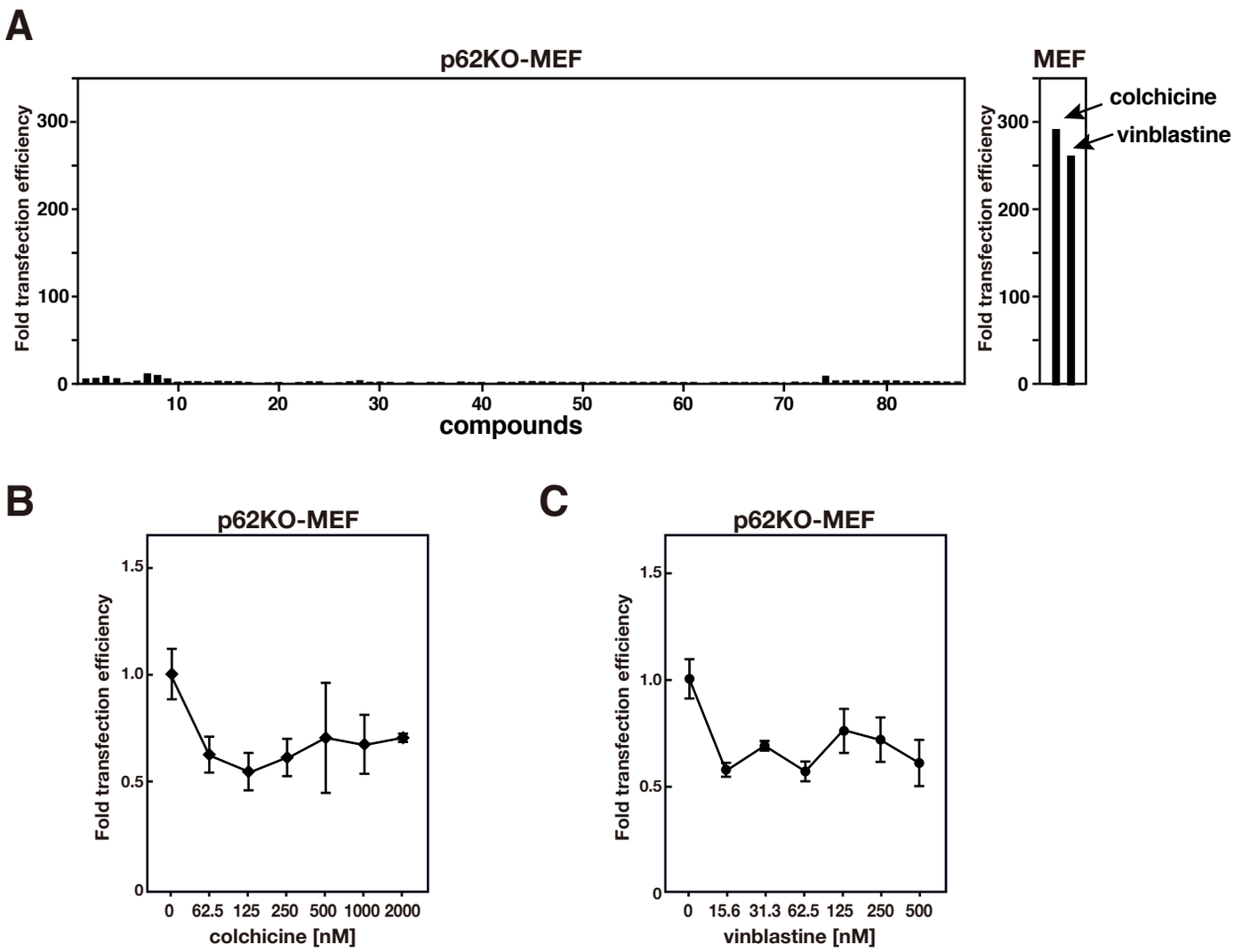
A
p62KO-MEF
Fold transfection efficiency
300
200
100
0
10
20
30
40
50
60
70
80
compounds
MEF
colchicine
vinblastine
B
p62KO-MEF
Fold transfection efficiency
1.5
1.0
0.5
0
0
62.5
125
250
500
1000
2000
colchicine [nM]
C
p62KO-MEF
Fold transfection efficiency
1.5
1.0
0.5
0
0
15.6
31.3
62.5
125
250
500
vinblastine [nM]

Fig. 4

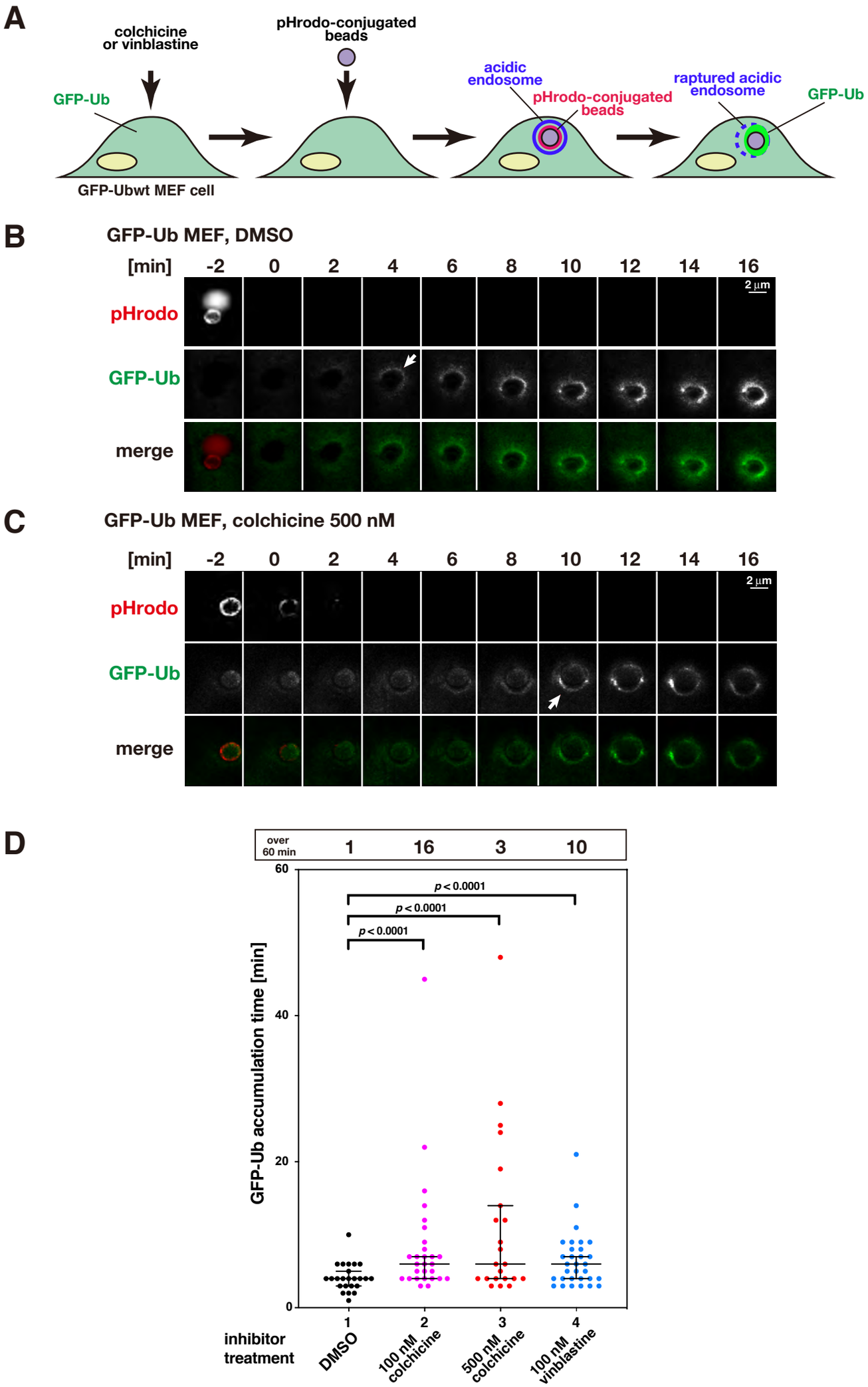
A
colchicine
or vinblastine
pHrodo-conjugated
beads
GFP-Ub
acidic
endosome
pHrodo-conjugated
beads
raptured acidic
endosome
GFP-Ub
GFP-Ubwt MEF cell
B
GFP-Ub MEF, DMSO
[min]
-2
0
2
4
6
8
10
12
14
16
2 μm
pHrodo
GFP-Ub
merge
C
GFP-Ub MEF, colchicine 500 nM
[min]
-2
0
2
4
6
8
10
12
14
16
2 μm
pHrodo
GFP-Ub
merge
D
over
60 min
1
16
3
10
p < 0.0001
p < 0.0001
p < 0.0001
GFP-Ub accumulation time [min]
60
40
20
0
1
2
3
4
inhibitor
treatment
DMSO
100 nM
colchicine
500 nM
colchicine
100 nM
vinblastine

Fig. 5

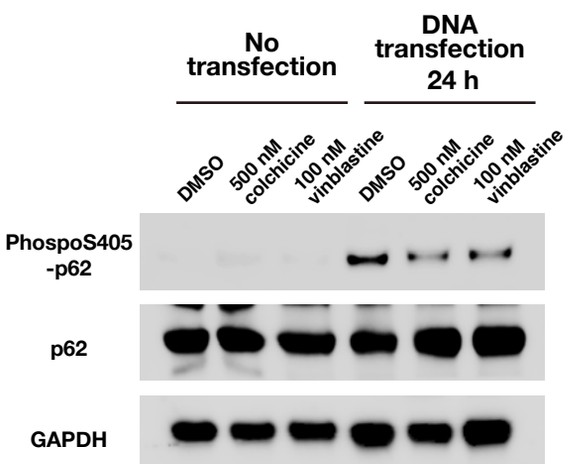
No transfection
DNA transfection 24 h
DMSO
500 nM colchicine
100 nM vinblastine
DMSO
500 nM colchicine
100 nM vinblastine
PhospoS405 -p62
p62
GAPDH

Supporting Information

Microtubule inhibitors identified through non-biased screening enhance DNA transfection efficiency by delaying p62-dependent ubiquitin recruitment

Megumi Tsuchiya[1#], Hidesato Ogawa[1#*], Kento Watanabe[1], Takako Koujin[2], Chie Mori[2], Kazuto Nunomura[3], Bangzhong Lin[3], Akiyoshi Tani[3], Yasushi Hiraoka[1,2], and Tokuko Haraguchi[1,2*]

List of contents:

Table S1

Figure S1

Figure S2

Figure S3

Table S1. Identification of 87 potential compounds for enhancement of transfection efficiency.

Rank	Structure	Name	Formula	Fold transfection efficiency in MEF	Fold cell viability in MEF	Fold transfection efficiency in p62KO-MEF	Fold cell viability in p62KO-MEF
1		PODOFILOX	C22 H22 O8	**297.24**	**64%**	**4.46**	**281%**
2		COLCHICINE	C22 H25 N O6	**294.20**	**95%**	**4.94**	**258%**
3		VINBLASTINE SULFATE	C46 H58 N4 O9 . H2 O4 S	**263.07**	**68%**	**6.90**	**318%**
4		DEOXYSAPPANONE B 7,4'-DIMETHYL ETHER	C18 H18 O5	**54.43**	**96%**	**4.72**	**95%**
5		VINCRISTINE SULFATE	C46 H56 N4 O10 . H2 O4 S	**46.77**	**40%**	**0.66**	**47%**
6		PICROPODOPHYLLIN ACETATE	C24 H24 O9	**35.46**	**34%**	**2.19**	**46%**
7		DOCETAXEL	C43 H53 N O14 . 3 H2 O	**33.78**	**72%**	**9.43**	**316%**
8		FENBENDAZOLE	C15 H13 N3 O2 S	**27.14**	**63%**	**7.83**	**337%**
9		FLUBENDAZOLE	C17 H13 F N2 O3	**21.35**	**71%**	**4.53**	**357%**
10			C18 H19 Cl F N O2	**8.77**	**59%**	**1.09**	**80%**
11			C18 H17 N O2 S2	**6.80**	**74%**	**1.80**	**68%**
12			C15 H26 N4 O5 S2	**6.19**	**89%**	**1.70**	**91%**
13		OXIBENDAZOLE	C12 H15 N3 O3	**4.64**	**45%**	**0.85**	**49%**
14		DEOXYSAPPANONE B 7,3'-DIMETHYL ETHER ACETATE	C20 H20 O6	**4.50**	**82%**	**2.07**	**85%**
15		PHENETHYL CAFFEATE (CAPE)	C17 H16 O4	**4.44**	**72%**	**1.63**	**89%**
16		MEBENDAZOLE	C16 H13 N3 O3	**3.01**	**95%**	**1.57**	**365%**
17		AZACITIDINE	C8 H12 N4 O5	**2.92**	**59%**	**0.93**	**67%**
18			C15 H10 Br F N2 O2	**2.84**	**96%**	**0.53**	**109%**
19			C15 H18 N4 O3	**2.52**	**97%**	**0.62**	**105%**
20		PIROCTONE OLAMINE	C14 H23 N O2 . C2 H7 N O	**2.04**	**40%**	**0.78**	**42%**
21			C18 H16 N2	**1.96**	**94%**	**0.38**	**102%**

22			C25 H21 N3 O5 S	**1.91**	**113%**	**0.76**	**101%**
23			C15 H29 N3 O2	**1.82**	**113%**	**1.52**	**116%**
24		ISOOSAJIN	C25 H24 O5	**1.59**	**62%**	**1.50**	**76%**
25		ALBENDAZOLE	C12 H15 N3 O2 S	**1.50**	**92%**	**0.62**	**222%**
26		PICROPODOPHYLLIN	C22 H22 O8	**1.49**	**93%**	**0.32**	**110%**
27		DEGUELIN(-)	C23 H22 O6	**1.44**	**36%**	**1.51**	**33%**
28		EPOXYGEDUNIN	C28 H34 O8	**1.37**	**77%**	**2.66**	**83%**
29		NISOLDIPINE	C20 H24 N2 O6	**1.32**	**91%**	**1.05**	**59%**
30		METHYLPREDNISOLONE SODIUM SUCCINATE	C26 H33 O8 . Na	**1.30**	**81%**	**1.24**	**65%**
31		METERGOLINE	C25 H29 N3 O2	**1.29**	**61%**	**0.93**	**54%**
32		THIOGUANINE	C5 H5 N5 S	**1.28**	**111%**	**0.45**	**106%**
33			C11 H15 Cl N2	**1.26**	**76%**	**1.02**	**88%**
34		TOLONIUM CHLORIDE	C15 H16 N3 S . Cl	**1.24**	**67%**	**0.49**	**45%**
35		MANIDIPINE HYDROCHLORIDE	C35 H38 N4 O6	**1.22**	**70%**	**0.90**	**51%**
36		PREGNENOLONE SUCCINATE	C25 H36 O5	**1.20**	**78%**	**0.85**	**73%**
37			C12 H13 Br N4 O S	**1.15**	**103%**	**0.56**	**102%**
38		MOMETASONE FUROATE	C27 H30 Cl2 O6	**1.14**	**80%**	**1.26**	**54%**
39		ESTRAMUSTINE	C23 H31 Cl2 N O3	**1.08**	**71%**	**0.79**	**77%**
40		PHENOLPHTHALEIN	C20 H14 O4	**1.07**	**76%**	**0.86**	**70%**
41		BROXYQUINOLINE	C9 H5 Br2 N O	**1.07**	**62%**	**0.63**	**58%**
42			C19 H30 Cl N O2	**1.06**	**101%**	**1.04**	**113%**
43		PHENOTHIAZINE	C12 H9 N S	**1.05**	**44%**	**0.86**	**64%**
44		PEUCENIN	C15 H16 O4	**1.05**	**54%**	**1.45**	**31%**

45		GANGALEOIDIN	C18 H14 Cl2 O7	**1.04**	**78%**	**1.71**	**71%**
46		7,3'-DIMETHOXYFLAVONE	C17 H14 O4	**1.01**	**84%**	**1.43**	**96%**
47		3-ACETYLGEDUNOL	C30 H40 O8	**1.00**	**102%**	**1.37**	**96%**
48		GARCINOLIC ACID	C38 H46 O9	**0.99**	**62%**	**0.88**	**54%**
49			C12 H12 N6 S2	**0.97**	**109%**	**0.94**	**126%**
50		SULBENTINE	C17 H18 N2 O S	**0.92**	**72%**	**0.63**	**73%**
51			C16 H16 Cl N3 O S	**0.92**	**85%**	**0.85**	**95%**
52		ISRADIPINE	C19 H21 N3 O5	**0.90**	**91%**	**0.80**	**71%**
53		DIHYDROGEDUNIN	C28 H36 O7	**0.90**	**37%**	**1.23**	**69%**
54		NITRENDIPINE	C18 H20 N2 O6	**0.88**	**72%**	**0.82**	**72%**
55		GEDUNIN	C28 H34 O7	**0.87**	**54%**	**1.23**	**80%**
56		PYRONARIDINE TETRAPHOSPHATE	C29 H32 Cl N5 O2 . 4 H3 O4 P	**0.87**	**79%**	**0.83**	**66%**
57		BENAZEPRIL HYDROCHLORIDE	C24 H28 N2 O5 . Cl H	**0.86**	**76%**	**1.06**	**60%**
58		PYRVINIUM PAMOATE	C26 H28 N3 . C23 H15 O6	**0.85**	**79%**	**1.46**	**147%**
59			C12 H12 N4 S	**0.83**	**101%**	**0.70**	**105%**
60			C16 H13 N3 O S2	**0.82**	**129%**	**0.80**	**137%**
61		SODIUM TETRADECYL SULFATE	C14 H29 O4 S . Na	**0.81**	**76%**	**0.83**	**69%**
62		DIENESTROL	C18 H18 O2	**0.81**	**92%**	**0.61**	**219%**
63		AMSACRINE	C22 H20 N2 O3 S	**0.81**	**38%**	**0.18**	**35%**
64		BISMUTH SUBSALICYLATE	C7 H5 Bi O4	**0.78**	**84%**	**0.84**	**48%**
65			C20 H16 N2 O3 S	**0.78**	**94%**	**0.86**	**104%**
66		AMINOETHOXYDIPHENYLBORANE	C14 H16 B N O	**0.76**	**94%**	**0.88**	**96%**
67			C11 H9 N O2	**0.75**	**97%**	**0.69**	**106%**

68		OXFENDAZOLE	C15 H13 N3 O3 S	**0.73**	**77%**	**0.80**	**78%**
69		CHLOROXINE	C9 H5 Cl2 N O	**0.71**	**87%**	**0.72**	**80%**
70		DIETHYLSTILBESTROL	C18 H20 O2	**0.66**	**105%**	**0.45**	**204%**
71		ESTRADIOL ACETATE	C20 H26 O3	**0.60**	**28%**	**1.21**	**49%**
72			C23 H26 O3	**0.55**	**104%**	**0.81**	**97%**
73			C22 H17 N3 O3	**0.44**	**110%**	**0.86**	**99%**
74			C15 H18 N4 O3 S3	**0.41**	**14%**	**7.11**	**37%**
75			C14 H14 N4 O S3	**0.07**	**203%**	**2.33**	**265%**
76			C15 H10 F3 N3 S	**0.07**	**257%**	**2.35**	**270%**
77			C15 H17 N3 O3	**0.07**	**199%**	**2.67**	**260%**
78			C16 H10 Br Cl2 N5	**0.06**	**203%**	**2.62**	**257%**
79			C20 H23 N O4 S	**0.06**	**203%**	**1.80**	**265%**
80			C17 H10 Cl N O4	**0.06**	**206%**	**2.52**	**262%**
81			C17 H19 Br O3	**0.06**	**222%**	**2.36**	**268%**
82			C15 H13 Cl N2 O4 S	**0.05**	**164%**	**1.75**	**155%**
83			C15 H14 Cl N3 O	**0.04**	**171%**	**1.52**	**163%**
84			C16 H13 Cl N4 O S2 . Cl H	**0.04**	**186%**	**1.59**	**162%**
85			C15 H13 Br N2 O2 S	**0.03**	**152%**	**1.58**	**150%**
86			C14 H18 N6 O2 S	**0.03**	**182%**	**1.26**	**190%**
87			C16 H18 N2 O2	**0.03**	**203%**	**1.27**	**188%**

Comparison of 87 compounds derived from the Osaka University compound library, showing their chemical structure, name, formula, transfection efficiency and cell viability in MEF cells and p62KO-MEF cells.

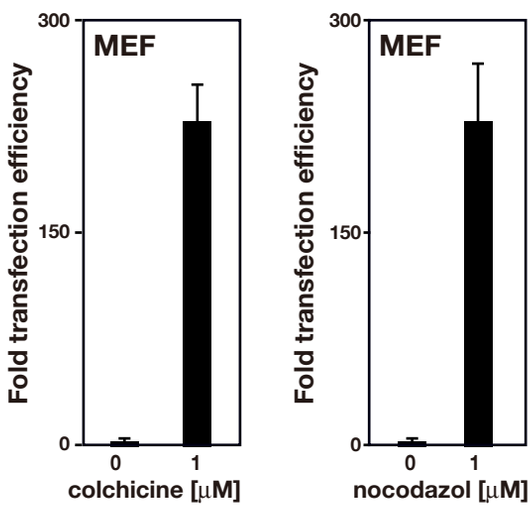

Fig. S1. Nocodazole increases gene transfection efficiency.

MEF cells were transfected with the pCMV-Luc plasmid for 28 h in the presence of 1 μM colchicine (left) and 1 μM nocodazole (right). DMSO was used as the negative control. Transfection efficiency was determined based on luciferase activity normalized to the cell viability. Bar graphs show the fold changes in transfection efficiency relative to the value from the control DMSO-treated cells. Each value is indicated as the mean ± SD of at least threeindependent experiments.

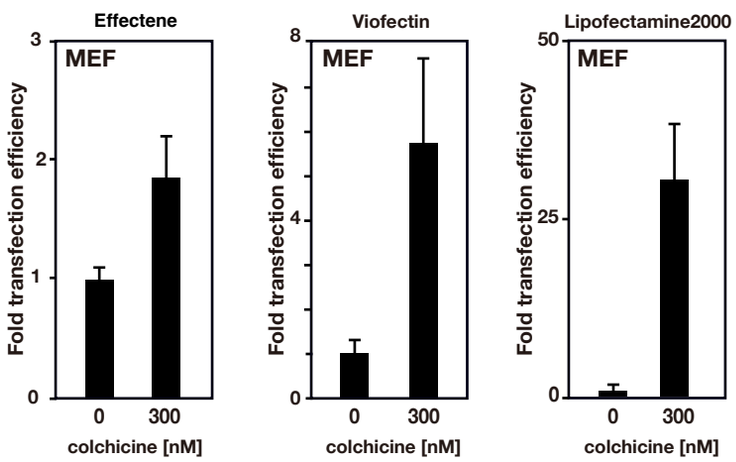

Fig. S2. Colchicine increases transfection efficiency for various transfection reagents.

MEF cells were transfected with the pCMV-Luc plasmid in the presence of 300 nM colchicine by using Effectene, Viofectin, or Lipofectamine 2000. DMSO was used as the negative control. Details of transfection procedures for each transfection reagent are described in the Experimental procedures. Bar graphs show the fold changes in transfection efficiency relative to the value from the control DMSO-treated cells. (mean ± SD of at least three independent experiments).

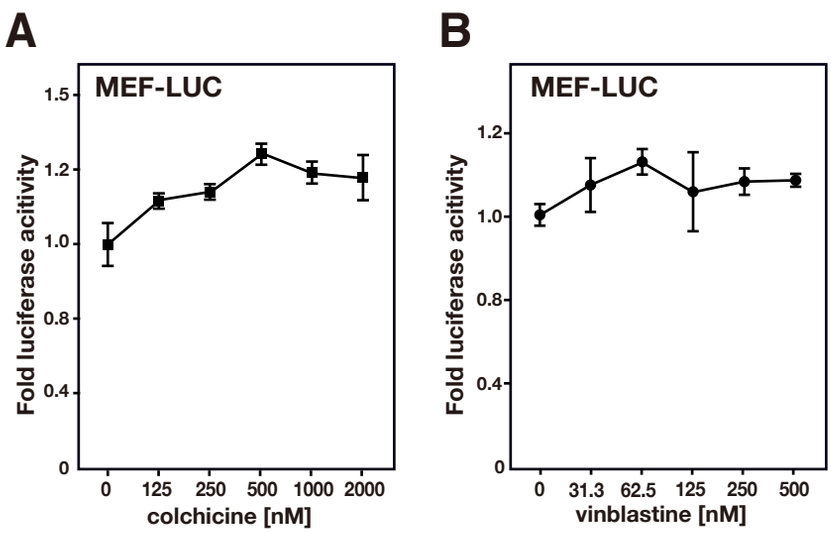

Fig. S3. Colchicine and vinblastine treatments do not affect the promoter activity of the luciferase gene.

(A, B) MEF cells stably expressing luciferase (MEF-LUC) were treated with the indicated concentrations of colchicine (A) or vinblastine (B). After incubation for 27 h, the luciferase activity of the cells was measured and normalized to cell viability. The graphs show the fold changes in luciferase activity relative to the value from the control DMSO-treated cells (indicated as mean ± SD of at least three independent experimental results).